Theory of the metastable injection-bleached $E3c$ center in GaAs

Peter A. Schultz * and Harold P. Hjalmarson
Sandia National Laboratories, Albuquerque, New Mexico 87185-1322, USA

(Received 5 April 2022; accepted 10 June 2022; published 23 June 2022)

The $E3$ transition in irradiated GaAs observed in deep level transient spectroscopy (DLTS) was recently discovered in Laplace-DLTS to encompass three distinct components. The component designated $E3c$ was found to be metastable, reversibly bleached under minority carrier (hole) injection, with an introduction rate dependent upon Si doping density. It is shown through first-principles modeling that the $E3c$ must be the intimate Si-vacancy pair, best described as a Si sitting in a divacancy Si_{vv}. The bleached metastable state is enabled by a doubly site-shifting mechanism: Upon recharging, the defect undergoes a second site shift rather returning to its original $E3c$-active configuration via reversing the first site shift. Identification of this defect offers insights into the short-time annealing kinetics in irradiated GaAs.

DOI: 10.1103/PhysRevB.105.224111

I. INTRODUCTION

Irradiation of GaAs reveals a rich variety of defect centers not observed in as-grown material [1]. The $EL2$ center appearing in as-grown material had been identified as the arsenic antisite $\mathrm{As_{Ga}}$—an As substituting for a Ga atom in the lattice—via computational modeling [2,3]. The identification of other radiation-induced defect centers in GaAs observed decades ago has also been accomplished via quantitatively reliable first-principles modeling [4] only relatively recently: the $E1$-$E2$ centers near the conduction band edge attributed to the divacancy and the $E3$ center observed by DLTS (deep level transient spectroscopy) at 0.3–0.4 below the conduction band edge (CBE) [1] assigned to the isolated As vacancy v_{As} [5]. Significant mysteries remain concerning primary defects (e.g., where is the v_{Ga}?) [4], and explicit knowledge of secondary defects and the initial reaction kinetics ensuing after irradiation in GaAs is minimal.

Recently, the $E3$ peak observed in DLTS was discovered by Taghizadeh *et al.* [6] to be composed of three distinct components using Laplace transform DLTS (L-DLTS) [7,8]. The primary $E3a$ component, presumably the v_{As}, was accompanied by two secondary components: an $E3b$ peak that appeared in intrinsic (undoped) material, and an $E3c$ component that was correlated with Si-doping level. The $E3c$ was determined to be metastable, and discovered to have the unusual property of becoming bleached upon minority carrier (hole) injection at low temperatures—the $E3c$ peak disappears—and then reappears upon annealing above 160 K. We use first-principles modeling to deduce that the $E3c$ center must be the intimate v_{Ga}-$\mathrm{Si_{As}}$ pair (Ga vacancy next to a Si on an As site), and propose a mechanism for the bleaching of the center via multiple site shifts. Hole injection induces a site shift in the defect, and recharging diverts the defect into a metastable twice-site-shifted form having no levels above midgap. The deduction of a plausible radiation-induced formation path for the defect provides additional evidence for the Si-vacancy pair model for the $E3c$ center in preference to other potential candidates. Discovery of this defect and the analysis of its formation provides useful insight into the unknown early-time kinetics after irradiation in GaAs that could be probed in new experiments.

*paschul@sandia.gov

Published by the American Physical Society under the terms of the Creative Commons Attribution 4.0 International license. Further distribution of this work must maintain attribution to the author(s) and the published article's title, journal citation, and DOI.

II. COMPUTATIONAL METHODS

The defect modeling follows the methods previously described in a comprehensive survey of intrinsic defects in GaAs [4] and in making the conclusive identification of the defects responsible for the $E1$-$E2$ and $E3$ centers [5]. The density functional theory (DFT) calculations are executed using the SeqQuest code [9], a pseudopotential code using Gaussian basis sets. A large-core ($Z = 3$) pseudopotential was found sufficient to describe the Ga atom for GaAs defects [10]. In the following, the Perdew-Burke-Ernzerhof (PBE) functional [11] is used in cubic supercell models ranging from 216-sites through 1000-sites, with a $2 \times 2 \times 2$ k-point sampling grid, without spin polarization. Spin polarization is observed to have minimal ($\lesssim 0.1$ eV) effect on defect energies. Unless otherwise noted, the analysis below quotes the 512-site supercell results, needed to fully converge the largest defects considered (extending across three lattice sites). Migration barriers are obtained via nudged elastic band (NEB) to obtain a minimum energy path [12], complemented by a modified Broyden method [13] to refine the candidate critical point configurations (saddle point barriers, and local minima) to reduce atomic forces to less than 0.0002 Ry/Bohr ($\sim$5 meV/Å). The self-consistent local moment countercharge (LMCC) approach [14,15] avoids the errors of a jellium neutralization. A

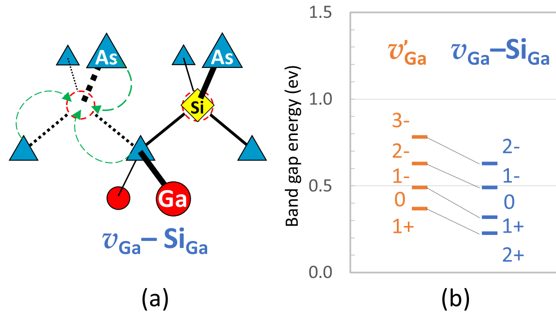

FIG. 1. The v_{Ga}-Si_{Ga} defect pair: (a) structure and (b) defect level diagram compared to the simple Ga vacancy (no site shift) v'_{Ga}. The arrows indicate possible site shifts of neighboring As into the Ga vacancy leading to potential metastable structures. This defect lacks levels above midgap that could be ascribed to the $E3c$ center.

modified-Jost model incorporates long-range (external to the supercell) screening into the total energy calculations. This successfully removes finite size errors, documented with the convergence of the results across supercells to a dilute bulk limit [16,17]. This approach has successfully predicted defect levels in Si to within 0.1 eV [16], and this 0.1 eV accuracy was instrumental in making earlier identifications of defect centers in GaAs [4,5].

III. RESULTS AND ANALYSIS

The L-DLTS experiments established that the $E3c$ center is created subsequent to electron irradiation, has a level 0.34 eV below the conduction band edge, $E_c - 0.34$ eV, that its concentration increases with increasing carrier density (Si doping), and that it anneals irreversibly at 525 K [6]. The $E3c$ disappears after hole injection at low temperatures, and is reversibly reintroduced upon annealing above 160 K (at zero bias). Each of these observations prove consequential to identify the defect responsible.

That $E3c$ anneals at the same temperature as the $E1$-$E2$ (vv) and primary $E3 = E3a$ (v_{As}) indicates involvement of a vacancy in the defect, while the dependence of the defect concentration upon doping level implicates involvement of a silicon atom [6]. These chemical fingerprints prompted Taghizadeh to speculate that the v_{Ga}-Si_{Ga} pair, schematically depicted in Fig. 1, might be responsible for the $E3c$ [6]. Their hypothesis aligned with an early proposal by Bondarenko *et al.* [18] associating $E3$ with this complex.

Our PBE-LMCC calculations predict v_{Ga}-Si_{Ga} has no levels near $E3c$. With a Si^+_{Ga} donor site near to a v_{Ga}, the levels of this defect complex should be expected to mimic the levels of the isolated v_{Ga}, but shifted deeper in the gap by the nearby charged Si^+ center. The v_{Ga} is known to have no levels above midgap, confirmed in calculations [4] that predict its defect levels lie in the lower half of the band gap, starting with the $v_{Ga}(3-/2-)$ charge transition near midgap. As shown in Fig. 1(b), the computed levels for v_{Ga}-Si_{Ga} indeed echo the isolated v'_{Ga} levels, shifted ~0.2 eV lower in the gap starting with the $(2-/1-)$. The numerical values for defect levels and formation energies are tabulated in Tables S-1 and S-2 within the Supplemental Material [19]. The v'_{Ga} specifies the simple form of the v_{Ga} while v^*_{Ga} denotes the site-shifted (As_{Ga}-v_{As}) form.

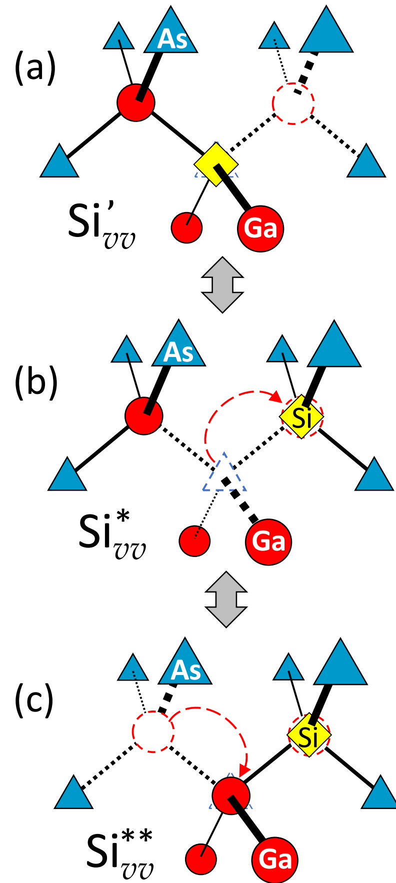

FIG. 2. The model for injection-bleached $E3c$ center as the Si_{vv} defect. (a) $Si'_{vv} = Si_{As}$-v_{Ga} pair, ground state in n-type (Si-doped) GaAs with its $(3-/2-)$ level leading to the $E3c$; (b) $Si^*_{vv} = v_{As}$-Si_{Ga}, obtained as the Si shifts sites upon hole injection and is the ground state for neutral and positive charge; (c) $Si^{**}_{vv} = v_{Ga}$-Ga_{As}-Si_{Ga}, a second site shift, of a Ga into the vacated As site, obtained upon recharging from the Si^*_{vv} and the ground state for $(1-)$ and $(2-)$. The Si^{**}_{vv} has no levels above midgap, and is the bleached form of the defect. To return to the Si'_{vv} and a visible $E3c$ requires traversing through the higher-energy Si^*_{vv} structure.

Similar to the site shifts seen for the simple Ga vacancy [4,20], the v_{Ga}-Si_{Ga} could experience site shifts leading to metastability as indicated by the arrows in Fig. 1. It is only with the $(2+)$ that the simulations indicate a site shift becomes more stable than the simple form, with the resulting $(1+/2+)$ defect level within 0.3 eV of the valence band edge. Upon recharging, this spontaneously shifts back to the simple defect. Finally, there is no plausible kinetic pathway to generate this defect pair from the primary defects following irradiation. The v_{Ga}-Si_{Ga} cannot be the responsible for the $E3c$.

The nearest-neighbor vacancy-Si pair, as depicted in Fig. 2, proves to be the more viable candidate. The v_{Ga}-Si_{Ga}, designated Si'_{vv}, is the ground state for the $(4-)$ and $(3-)$ charge states and is found to be locally stable in charge states down to $(2+)$, as depicted in the level diagram in Fig. 3. A $(4-/3-)$ charge transition level is predicted near the CBE. The computed $Si'_{vv}(3-/2-)$ level is 0.23 eV

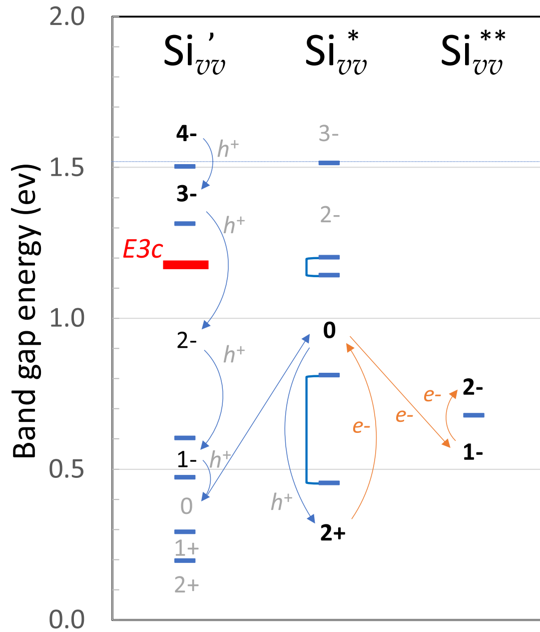

FIG. 3. Structure-resolved defect level diagram for the Si_{vv} illustrating the bleaching mechanism. The hole injection into the Si'_{vv} drives the defect to the (0) charge, at which point the Si shifts with minimal barrier (<0.1 eV) to form the more stable (by 0.7 eV) $Si^*_{vv}(0)$. Upon recharging with electrons, the capture of an electron converts from $Si^*_{vv}(0)$ to the lower-energy $Si^{**}_{vv}(1-)$ with small $\sim$0.1 eV barrier, which can then trap one more electron to form the $Si^{**}_{vv}(2-)$. The measured $E3c$ is assigned to the $Si'_{vv}(3-/2-)$ transition. The Si^{**}_{vv} is invisible above midgap, and needs to overcome a barrier over $Si^*_{vv}(2-)$ to capture additional electrons and return to the Si'_{vv} structure and a visible $E3c$.

below the CBE (0.36 including spin polarization). We propose this transition is responsible for the $E3c$ center seen in L-DLTS.

Like the isolated As vacancy (a v_{As} site-shift metastability leads to the primary $E3$ DLTS signal) [4,5], the v_{Ga}-$\mathrm{Si}_{\mathrm{As}}$ is susceptible to a site shift. This site shift becomes progressively more favorable as electrons are removed. Shift of the Si into the vacant v_{Ga} site, designated as Si^*_{vv}, is locally stable for charge states ranging from (3−) down to (2+). A $Si^*_{vv}(4-)$ is unstable and the Si spontaneously shifts back into the Si'_{vv}. The $Si^*_{vv}(3-)$ and (2−) are only marginally locally metastable with very small (<0.1 eV) barriers to shift back to the lower energy Si'_{vv} structure. See Tables S-3 and S-4 in the Supplemental Material [19] for tabulations of the formation energies and barriers. This site-shifted Si^*_{vv} structure becomes more stable than Si'_{vv} for charge (1−) and becomes increasingly more stable as more electrons are removed. However, this Si-shifted metastability alone cannot be not responsible for the observed bleaching under hole injection. Upon recharging, a Si^*_{vv} recaptures electrons and would shift back to Si'_{vv} with a minimal (0.01 eV) computed barrier at (3−).

The crucial process is a second site shift, of a neighboring Ga into the v_{As}, to form a $\mathrm{Si}_{\mathrm{Ga}}$-$\mathrm{Ga}_{\mathrm{As}}$-$v_{\mathrm{Ga}}$ complex designated Si^{**}_{vv} in Fig. 2. This is the most stable structure for Si_{vv} in the (1−) and (2−) charge states, and Si^{**}_{vv} is locally stable only in those charge states. A $Si^{**}_{vv}(3-)$ state lies slightly above the CBE in these calculations. The $Si^{**}_{vv}(0)$ structure is unstable and spontaneously shifts back to the ground state $Si^*_{vv}(0)$. The $Si^{**}_{vv}(2-/1-)$ level is below midgap, at $\lesssim$0.7 eV above the VBE. This second site shift provides the mechanism for the observed bleaching of $E3c$.

The second-site-shift mechanism for bleaching is illustrated in the level diagrams of Fig. 3. The Si'_{vv} captures injected holes until it becomes neutral, at which point it converts to the lower energy site-shifted $Si^*_{vv}(0)$ (overcoming a trivial <0.1 eV barrier). Upon recharging, when the $Si^*_{vv}(0)$ captures an electron, instead of retracing its path to shift back to the (higher-energy) $Si^*_{vv}(1-)$, a Ga neighbor shifts into the As vacancy to form the double-site-shifted ground state $Si^{**}_{vv}(1-)$ structure. For both the (1−) and (2−) the Si^{**}_{vv} is more stable than Si^*_{vv}, by 0.1 and 0.6 eV, respectively. There is only a small $\sim$0.1 eV barrier for this second site shift. Conversely, the computed barrier for $Si^{**}_{vv}(2-)$ to reverse this second site shift is $\gtrsim$0.7 eV, leaving the defect trapped in this double-shifted configuration at low temperatures. With its highest $Si^{**}_{vv}(2-/1-)$ level at VBE + 0.7 eV, the $E3c$ peak has disappeared. Recovery of the $E3c$ center occurs when the temperature is raised sufficiently to overcome the barrier to shift back to the Si^*_{vv} configuration. This quickly captures additional electrons into defect levels drawn down into the gap and the atomic configuration continues to unshift with small barriers to the $E3c$-active (and lowest energy) Si'_{vv} in the (3-) and (4-) charge states.

Deducing the creation of this defect provides insight into the initial annealing kinetics. The simplest model would hypothesize this is a primary displacement defect: a vacancy created next to an $\mathrm{Si}_{\mathrm{Ga}}$ dopant. Just as for the v_{Ga}-$\mathrm{Si}_{\mathrm{Ga}}$ candidate above, the number of Si dopants is much smaller than the number of As atoms, and could not yield an $E3c$ signal comparable to the $E3a$ (due to primary As displacements). The $\mathrm{Si}_{\mathrm{Ga}}$ dopant is immobile, as are the vacancies in GaAs (at these temperatures) [21,22]. This eliminates a model proposing coalescence of the two via simple migration. The remaining plausible reaction pathway to form the intimate vacancy-silicon pair is for a mobile Si interstitial to find and enter a divacancy: $\mathrm{Si}_{vv} \leftarrow vv + \mathrm{Si}_i$

The divacancy had been determined to be a prominent primary displacement damage defect [4,5]. The Si interstitial cannot be from a primary displacement event, again the number density of $\mathrm{Si}_{\mathrm{Ga}}$ dopants is too small for the population of $E3c$ to descend from radiation-displaced Si dopants. This mobile Si_i must be the result of a kick-out of a $\mathrm{Si}_{\mathrm{Ga}}$ dopant by a mobile native interstitial i. It cannot be the As_i, the calculations predict the $(\mathrm{AsSi})_{\mathrm{Ga}}$ is a strongly bound complex. It must be a Ga_i that kicks out a mobile Si_i, leaving behind a healed lattice: $\mathrm{Si}_i \leftarrow \mathrm{Si}_{\mathrm{Ga}} + \mathrm{Ga}_i$

The native interstitials are primary defects. The As_i has been hypothesized to migrate athermally [1,4,23] while the Ga_i has been determined to have a modest ($\lesssim$1 eV) thermal migration barrier [4,24]. The current analysis indicates that it is the Ga_i that must displace the Si atom from its dopant site. The L-DLTS measurements resolving the $E3c$ had been performed after annealing samples to room temperature [6]. We propose that an *in situ* experiment limiting the annealing to the 180 K necessary to accomplish the measurement of the $E3c$, and probing annealing temperatures from there to

300 K, could be revealing about the process of activating this hypothesized mobile Si_i.

IV. CONCLUSIONS

In summary, the $E3c$ is identified as an intimate Si-vacancy pair, a defect best designated as Si_{vv}, through good agreement with the computed defect level (within ∼0.1 eV) and a detailed mechanism leading to bleaching after hole injection. This analysis confirms the important role of site shifts in vacancy-involved III-V defects. The attribution is further supported by the deduction of a plausible formation mechanism after irradiation, which provides additional evidence supporting the finding that vv is a common primary displacement damage defect [5]. This identification indicates that Si_i and Ga_i must be mobile at low temperatures in n-type GaAs. The discovery of $E3c$ through better resolved L-DLTS experiments [6], coordinated with more quantitatively accurate DFT methods to identify defects and infer reaction mechanisms reveals an indirect means to experimentally probe features of otherwise inaccessible early-time defect kinetics in irradiated GaAs.

ACKNOWLEDGMENTS

We are grateful to F. Taghizadeh for clarifying aspects of their L-DLTS experiments for GaAs. Sandia National Laboratories is a multimission laboratory managed and operated by National Technology and Engineering Solutions of Sandia, LLC, a wholly owned subsidiary of Honeywell International, Inc., for the U.S. Department of Energy's National Nuclear Security Administration under Contract No. DE-NA0003525. This paper describes objective technical results and analysis. Any subjective views or opinions that might be expressed in the paper do not necessarily represent the views of the U.S. Department of Energy or the United States Government.

[1] J. C. Bourgoin, H. J. Bardeleben, and D. Stiévenard, Native defects in gallium arsenide, J. Appl. Phys. **64**, R65 (1988).
[2] J. Dabrowski and M. Scheffler, Theoretical Evidence for and Optically Inducible Structural Transition of the Isolated As Antisite in GaAs: Identification and Explanation for the $EL2$, Phys. Rev. Lett. **60**, 2183 (1988).
[3] D. J. Chadi and K. J. Chang, Metastability of the Isolated Arsenic-Antisite Defect in GaAs, Phys. Rev. Lett. **60**, 2187 (1988).
[4] P. A. Schultz and O. A. von Lillienfeld, Simple intrinsic defects in gallium arsenide, Modelling Simul. Mater. Sci. Eng. **17**, 084007 (2009).
[5] P. A. Schultz, The $E1$-$E2$ center in gallium arsenide is the divacancy, J. Phys.: Condens. Matter **27**, 075801 (2015).
[6] F. Taghizadeh, K. Ostvar, F. D. Auret, and W. E. Meyer, Laplace DLTS study of the fine structure and metastability of the radiation-induced E3 defect level in GaAs, Semicond. Sci. Technol. **33**, 125011 (2018).
[7] L. Dobaczewski and P. Kaczor, Laplace transform deep-level transient spectroscopic studies of defects in semiconductors, J. Appl. Phys. **76**, 194 (1994).
[8] L. Dobaczewski, A. R. Peaker, and K. B. Nielson, Laplace-transform deep-level spectroscopy: The technique and its applications to the study of point defects in semiconductors, J. Appl. Phys. **96**, 4689 (2004).
[9] P. A. Schultz, SeqQuest code (unpublished), see https://dft.sandia.gov/Quest/.
[10] P. A. Schultz and A. H. Edwards, Modeling charged defects inside density functional theory band gaps, Nucl. Instrum. Methods Phys. Res., Sect. B **327**, 2 (2014).
[11] J. P. Perdew, K. Burke, and M. Ernzerhof, Generalized Gradient Approximation Made Simple, Phys. Rev. Lett. **77**, 3865 (1996).
[12] H. Jonsson, G. Mills, and K.W. Jacobsen, Nudged elastic band method for finding minimum energy paths of transitions, *Classical and Quantum Dynamics in Condensed Phase Simulations* (World Scientific, Singapore, 1998), p. 385.
[13] D.D. Johnson, Modified Broyden's method for accelerating convergence in self-consistent calculations, Phys. Rev. B **38**, 12807 (1988).
[14] P. A. Schultz, Local electrostatic moments and periodic boundary conditions, Phys. Rev. B **60**, 1551 (1999).
[15] P. A. Schultz, Charged Local Defects in Extended Systems, Phys. Rev. Lett. **84**, 1942 (2000).
[16] P. A. Schultz, Theory of Defect Levels and the "Band Gap Problem" in Silicon, Phys. Rev. Lett. **96**, 246401 (2006).
[17] P. A. Schultz, R. M. Van Ginhoven, and A. H. Edwards, Theoretical study of intrinsic defects in cubic silicon carbide 3C-SiC, Phys. Rev. B **103**, 195202 (2021).
[18] V. Bondarenko, J. Gebauer, F. Redmann, and R. Kraus-Rehberg, Vacancy formation in GaAs under different equilibrium conditions, Appl. Phys. Lett. **87**, 161906 (2005).
[19] See Supplemental Material at http://link.aps.org/supplemental/10.1103/PhysRevB.105.224111 for numerical tabulation of data presented in figures and results discussed in the text.
[20] G. A. Baraff and M. Schlüter, Bistability and Metastability of the Gallium Vacancy in GaAs: Actuator of the $EL2$? Phys. Rev. Lett. **55**, 2340 (1985).
[21] F. El-Mellouhi and N. Mousseau, Charge-dependent migration pathways for the Ga vacancy in GaAs, Phys. Rev. B **74**, 205207 (2006).
[22] F. El-Mellouhi and N. Mousseau, Ab initio characterization of arsenic vacancy diffusion pathways in GaAs with SIESTA-ART, Appl. Phys. A **86**, 309 (2007).
[23] A. F. Wright and N. A. Modine, Migration processes of the As interstitial in GaAs, J. Appl. Phys. **120**, 215705 (2016).
[24] J. T. Schick and C. G. Morgan, Gallium interstitial contributions to diffusion in gallium arsenide, AIP Adv. **1**, 032161 (2011).